

# Enhanced Receivers for Interference Cancellation in 3G Systems

Petr KEJÍK<sup>1</sup>, Stanislav HANUS<sup>1</sup>

<sup>1</sup> Dept. of Radio Electronics, Brno University of Technology, Purkyňova 118, 612 00 Brno, Czech Republic

xkejik00@stud.feec.vutbr.cz, hanus@feec.vutbr.cz

**Abstract.** *Interference cancellation and multiuser detection in CDMA systems are still actual research topics. These techniques enable us to deal with interference and to increase system capacity. In this paper, a so-called Generalized RAKE receiver, an Uplink generalized multiuser detection and a Blind adaptive multiuser detection are described. These algorithms are compared with conventional receivers and their properties are verified via simulations. The results imply that some of these algorithms are able to overcome the performance of the conventional receivers.*

## Keywords

Interference cancellation, multiuser detection, CDMA, G-RAKE.

## 1. Introduction

Whereas 2G (2<sup>nd</sup> generation) systems are limited due to a lack of radio resources (number of radio channels), 3G (3<sup>rd</sup> generation) systems are limited due to interference. Interference cancellation and multiuser detection enable increasing the number of users in the system and thus they increase system capacity. In the case of uplink it is possible to use quite simple but effective multiuser detection, because a base station (Node B) has information about all users. Another possibility how to increase system capacity is to use spatial diversity. Uplink generalized multiuser detection will be briefly described below.

In the case of downlink it is not so easy to apply multiuser detection, because a mobile station (User equipment) has limited information about other users. It is also not so easy to use the spatial diversity technique in this case, because of the mobile station proportions and power supply limitations. Generalized RAKE receiver and Blind adaptive multiuser detection will be described below, and their properties will be verified via simulations.

## 2. G-RAKE Receiver

G-RAKE receiver is a downlink receiver for CDMA systems developed by Ericsson, see [1]. The receiver was

described in [1] and [2], on which this section is based. Another approach to interference cancellation can be found in [3], [4], [5] and [6], for example.

G-RAKE receiver (as well as a conventional RAKE receiver) can mitigate multipath and, moreover, to suppress intracell interference. This type of interference appears due to the loss of orthogonality between signals because of multipath propagation. G-RAKE is essentially based on the matched filter theory for colored noise. G-RAKE has the same structure as a RAKE receiver but it may have more fingers. Fingers may be at different delays and use different combining coefficients. Intracell interference is modeled as colored Gaussian noise and intercell interference is modeled as white Gaussian noise. The receiver structure is illustrated in Fig. 1. It consists of  $J$  fingers. Each finger is correlated to a different delayed component of the received signal  $r(t)$ . This signal first passes through a SRRC (Square Root Raised Cosine) filter. It is assumed that despreading code  $c_{k,i}$  is a product of the channel spreading code, which is specific for every user, and the scrambling sequence, which is specific for each base station. Spreading sequences are mutually orthogonal; a complex scrambling sequence is composed of two random binary sequences. Finger outputs  $y(d_j)$  are multiplied by combining coefficients  $w_j$  and added up to form decision statistic  $z$  for symbol detection (depends on the modulation used: BPSK or QPSK).

### 2.1 Finger Delays

Finger delay placement is still an open question. Two suggestions can be found in [1]:

- The first possibility is to use plenty of finger delay combinations and then simply choose the one which provides the best results (maximum SNR). This method is fairly complex but it enables achieving the best results.
- The second one, so-called symmetrical strategy method, will be explained on the following example. It is assumed there is a channel which has two rays. The dominant path is on the 0 position and the second path on the  $\tau$  position. G-RAKE has three fingers: at 0,  $\tau$  and  $-\tau$  position, the last one being symmetrical to the  $\tau$  position.

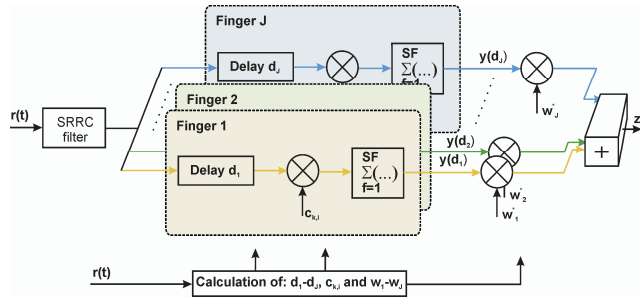


Fig. 1. Schematic structure of G-RAKE receiver.

## 2.2 Combining Coefficients

Combining coefficients were derived by using the maximum likelihood approach. Its detailed derivation was introduced in [1], but in this paper only the main points are presented. The vector of finger outputs  $\mathbf{y}$  can be expressed as:

$$\mathbf{y} = \mathbf{h}s + \mathbf{u}. \quad (1)$$

Vector  $\mathbf{u}$  models noise and interference,  $s$  is the desired transmitted symbol and  $\mathbf{h}$  is the modification of channel impulse response. According to [1], vector of combining coefficients  $\mathbf{w}$  is equal to

$$\mathbf{w} = \mathbf{R}_u^{-1} \mathbf{h} \quad (2)$$

where  $\mathbf{R}_u = E[\mathbf{u}\mathbf{u}^H]$  is the correlation matrix of noise vector  $\mathbf{u}$ ,  $[-]^H$  denotes the Hermitian transpose. The noise vector models intersymbol interference, an interference that appears because of the loss of orthogonality between serving cell signals and white Gaussian noise. The correlation matrix can be expressed as a sum of several components

$$\mathbf{R}_u = E_0 \mathbf{R}_{ISI} + E_I \mathbf{R}_{MUI} + N_0 \mathbf{R}_n \quad (3)$$

where  $E_0$ ,  $E_I$  and  $N_0$  are the symbol energies of the respective signal components. Matrixes  $\mathbf{R}$ , see (8-10), are squared; their dimension depends only on the number of fingers ( $J \times J$  dimension). The finger outputs are multiplied by the combining coefficients and added up to form decision statistic  $z$

$$z = \mathbf{w}^H \mathbf{y}. \quad (4)$$

The combining coefficients are calculated by using (2). Particular components of that equation can be calculated by using the following equations

$$\mathbf{h} = \sqrt{E_0} \mathbf{y}_d \quad (5)$$

where  $\mathbf{y}_d$  is the discrete form of the desired received signal (the desired component of received signal). Regarding (3), the following equations are examples of calculating element  $\mathbf{R}(d_1, d_2)$ , see [1]

$$y_d(d_1) = \sum_{l=0}^{L-1} g_l R_p(d_1 - \tau_l) \quad (6)$$

where  $L$  is the number of channel paths,  $g_l$  and  $\tau_l$  are the complex channel coefficient and delay for the  $l^{\text{th}}$  path, respectively.  $R_p(t)$  is the autocorrelation function of the chip pulse shape  $p(t)$

$$R_p(t) = \int_{-\infty}^{\infty} p(t+\tau) p^*(\tau) d\tau. \quad (7)$$

Particular components of equation (3) can be calculated by using the following simplified equations, see [1]

$$\begin{aligned} R_{ISI}(d_1, d_2) &= \frac{1}{SF^2} \sum_{l=0}^{L-1} \sum_{q=0}^{L-1} \sum_{\substack{i=-\infty \\ i \neq 0}}^{\infty} g_l g_q^* \\ &\times \sum_{m=1-SF}^{SF-1} (SF - |m|) \\ &\times R_p(d_1 + mT_c - iSF - \tau_l) \\ &\times R_p^*(d_2 + mT_c - iSF - \tau_q) \end{aligned} \quad (8)$$

$$\begin{aligned} R_{MUI}(d_1, d_2) &= \frac{1}{SF^2} \sum_{l=0}^{L-1} \sum_{q=0}^{L-1} g_l g_q^* \\ &\times \sum_{i=-\infty}^{\infty} \sum_{m=1-SF}^{SF-1} (SF - |m|) \\ &\times R_p(d_1 + mT_c - iT - \tau_l) \\ &\times R_p^*(d_2 + mT_c - iT - \tau_q) \\ &\times (1 - \delta(m)\delta(i)) \end{aligned} \quad (9)$$

$$\bar{R}_n(d_1, d_2) = R_p(d_1 - d_2) \quad (10)$$

where  $SF$  is the spreading factor and  $T_c$  is the chip duration. According to Fig. 1, to calculate the combining coefficients it is necessary for the receiver to know the radio channel parameters, spreading and scrambling codes, autocorrelation of the chip pulse shape, and finger placement.

## 2.3 Simulation Parameters

A mathematical model of UMTS downlink was created in MATLAB. This model was based on [1] and 3GPP specifications, see [7]. The channel (its baseband equivalent) was assumed to be time invariant with three paths. All paths were separated with one chip (delays were 0, 1 and 2 chip periods) and their relative amplitudes were 0, -3 and -8 dB. All simulations were done with these parameters: number of active users in downlink = 1 up to 32, spreading factor  $SF = 32$ , one realization with 600 up to 2400 transmitted bits. Parameter  $i$ , which is included in (8) and (9), was established within the range  $\langle -10, 10 \rangle$ . All simulation results (figures) were approximated by polynomial functions.

Fig. 2 shows the simplified block scheme of the model designed. The binary data of each user are QPSK

mapped and then the channel and scrambling codes are applied. Signals of all users in the cell are added up and passed through SRRC filter with the roll-off factor = 0.22. The obtained signal passes through channel model and the received signal  $r(t)$  is processed by G-RAKE and RAKE receivers.

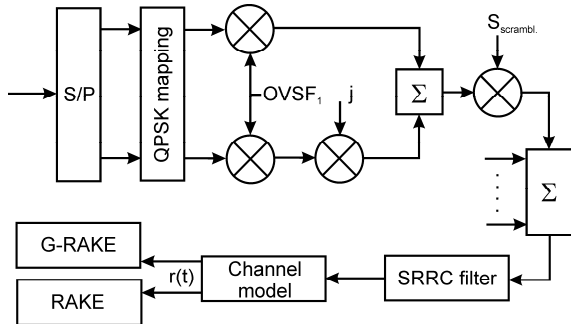


Fig. 2. Schematic structure of downlink simulated model.

### 3. Multiuser Detection

The problem with interference is especially significant in the case of uplink. Every UE (User Equipment) uses its unique scrambling code. These codes are not orthogonal, so interference appears. Whereas downlink is limited by the number of orthogonal codes, uplink is interference limited. Multiuser techniques could be used to improve received signal detection and thus increase system capacity. Uplink multiuser detection and generalized uplink multiuser detection are introduced in this section, which is based on [8]. Another approach to multiuser detection can be found in [9], [10] and [11], for example.

#### 3.1 Uplink Multiuser Detection

Uplink multiuser detection (UMUD) refers to joint detection of all users in the cell of interest. It enables suppressing intracell interference. The base station (Node B) receives the signal

$$\mathbf{r} = \mathbf{A} \cdot \mathbf{d} + \mathbf{n} \quad (11)$$

where  $\mathbf{r}$  denotes the vector of received samples,  $\mathbf{A}$  is the system matrix,  $\mathbf{d}$  is the vector of multiplexed transmitted symbols of all users in the cell of interest, and  $\mathbf{n}$  is the vector of AWGN with  $\sigma_n^2$  variance. The system matrix is composed of vectors which correspond to the spreading and scrambling codes. These vectors are convolved with their respective channel impulse responses. The principle of symbol multiplexing and the system matrix generation are shown by using a simple example. It is assumed there are 3 users. Each user is defined by their vector, so there are 3 vectors:  $\mathbf{a}$ ,  $\mathbf{b}$  and  $\mathbf{c}$ . Each vector is, for simplification, defined by only 2 elements. Each user transmits only 2 bits (or dibits)  $d_{k1}$  and  $d_{k2}$ . If noise is neglected, then equation (11) can be expressed in the form

$$\begin{bmatrix} r_1 \\ r_2 \\ r_3 \end{bmatrix} = \begin{bmatrix} a_1 & b_1 & c_1 & 0 & 0 & 0 \\ a_2 & b_2 & c_2 & 0 & 0 & 0 \\ 0 & 0 & 0 & a_1 & b_1 & c_1 \\ 0 & 0 & 0 & a_2 & b_2 & c_2 \end{bmatrix} \times \begin{bmatrix} d_{11} \\ d_{21} \\ d_{31} \\ d_{12} \\ d_{22} \\ d_{32} \end{bmatrix} \quad (12)$$

In the ideal case, a perfect knowledge of channel, spreading and scrambling codes and zero noise are assumed. Symbol recovery could be done by using the inverse matrix

$$\mathbf{d}_r = \mathbf{A}^{-1} \cdot \mathbf{r}. \quad (13)$$

In an unideal case, the recovered vector of transmitted symbols  $\mathbf{d}_r$  can be found by using the MMSE (Minimum Mean Square Error) approach, which leads, according to [8], to

$$\mathbf{d}_r = (\mathbf{A}^H \cdot \mathbf{A} + \sigma^2 \cdot \mathbf{I})^{-1} \mathbf{A}^H \cdot \mathbf{r} \quad (14)$$

where  $\mathbf{I}$  is the identify matrix,  $\sigma^2 = \sigma_n^2 + \sigma_i^2$ , where  $\sigma_i^2$  is the variance of AWGN caused by users from neighboring cells.

#### 3.2 Uplink Generalized Multiuser Detection

The UMUD regards signals from other cells as noise. The UGMUD (Uplink Generalized Multiuser Detection) takes these signals as an intracell signal, so it includes not only intracell but also intercell interference. Equation (11) turns into

$$\mathbf{r} = \sum_{i=1}^J \mathbf{A}_i \cdot \mathbf{d}_i + \mathbf{n} = \mathbf{G} \cdot \mathbf{d} + \mathbf{n}. \quad (15)$$

System matrix  $\mathbf{G}$  includes system matrixes of neighboring  $J$  cells

$$\mathbf{G} = [\mathbf{A}_1 \quad \mathbf{A}_2 \quad \mathbf{A}_3 \quad \dots \quad \mathbf{A}_J] \quad (16)$$

where  $\mathbf{d}_i$  is the vector of multiplexed data of all users under consideration

$$\mathbf{d} = [\mathbf{d}_1^T \quad \mathbf{d}_2^T \quad \mathbf{d}_3^T \quad \dots \quad \mathbf{d}_J^T]^T. \quad (17)$$

Equation (14) turns into

$$\mathbf{d}_r = (\mathbf{G}^H \cdot \mathbf{G} + \sigma^2 \cdot \mathbf{I})^{-1} \mathbf{G}^H \cdot \mathbf{r}. \quad (18)$$

The algorithm requires the knowledge of propagation channels from all users to the desired base station and all spreading and scrambling codes of all users.

#### 3.3 Simulation Parameters

The program used for the simulation of the above multiuser detection algorithms is a modified version of the

program for downlink, see subsection 2.3. The system model is shown in Fig. 3. A few simplifications were done: Signal spreading is the same as the UMTS uplink while scrambling is the same as for the downlink. The system matrixes  $\mathbf{G}$  and  $\mathbf{A}$  are quite complex to design, so there are a few simplifications again: All channel models for all users were assumed to be the same,  $\sigma^2$  was set to the value 0.1. The channel (its baseband equivalent) was assumed to be time invariant with three paths. All paths were separated with one chip (delays were 0, 1 and 2 chip periods) and their relative amplitudes were 0, -10 and -20 dB. Note that the multipath scenario (respective channel impulse responses) was not included in the system matrixes in this paper. All simulations were done with these parameters: spreading factor  $SF = 32$ , 10000 realizations. All simulation results (figures) were approximated by polynomial functions.

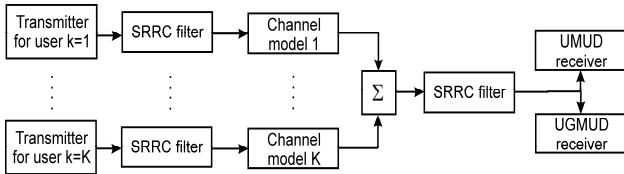


Fig. 3. Schematic structure of simulated model.

## 4. Blind Adaptive Multiuser Detection

Blind adaptive multiuser detection (denoted BMUD) will be introduced in this section. The algorithm was described in [12], where its more detailed description and derivation of several equations can be found (That is not the purpose of this paper.). This section is based on the above source. The proposed algorithm is quite simple. It requires only the same information as a conventional matched filter (Hence blind multiuser detection.). The algorithm could be implemented in uplink and in downlink. The algorithm (detector) is based on the minimization of the mean output energy (by using  $\mathbf{x}_1$ , see (20)). The impulse response of the detector is decomposed into two orthogonal components, see Fig. 4:

- Spreading sequence of the user of interest  $\mathbf{s}_1$ .
- Adaptive component  $\mathbf{x}_1$ , which is orthogonal with respect to  $\mathbf{s}_1$ .

### 4.1 Detector Derivation

The conventional matched filter is based on the equation

$$\underline{b} = \text{sgn}\left(\sum_{j=1}^{SF} \mathbf{y}[i, j] \cdot \mathbf{c}_1[j]\right) \quad (19)$$

where  $\underline{b}$  is the estimated transmitted data symbol of the user of interest,  $\mathbf{y}[i, j]$  is a part of the received signal (the vector of received samples in the  $i^{\text{th}}$  observation interval of

a length equal to the spreading factor) and  $\mathbf{c}_1 = \mathbf{s}_1$  (spreading sequence of the user of interest). The impulse response of BMUD is decomposed into two orthogonal components

$$\mathbf{c}_1 = \mathbf{s}_1 + \mathbf{x}_1. \quad (20)$$

BMUD was derived from MMSE (Minimum Mean Square Error) multiuser detector and also from minimum output energy detector. This could be viewed as a sensible approach. The output energy of the detector is a sum of the energy due to desired signal and the energy due to interference. It is assumed that interference is uncorrelated with the desired signal.

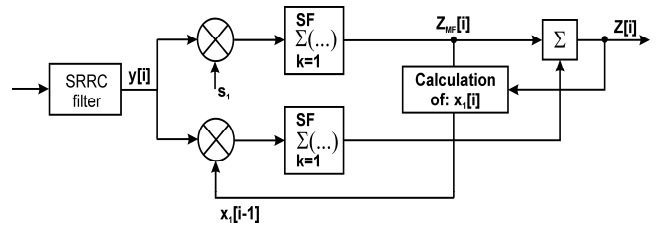


Fig. 4. Schematic structure of BMUD detector.

It is obvious that the impulse response has to be decomposed into two orthogonal components. In other cases, output energy minimization will result in a simple but impracticable solution:  $\mathbf{c}_1 = 0$ . It is assumed that receiver treats a received waveform (sampled)  $\mathbf{y}[i] \in [0, T]$  in the  $i^{\text{th}}$  interval  $[iT, iT+T]$ ,  $T$  is the data symbol duration. The following equations correspond with Fig. 4

$$Z_{MF}[i] = \sum_{j=1}^{SF} \mathbf{y}[i, j] \cdot \mathbf{s}_1[j], \quad (21)$$

$$Z[i] = \sum_{j=1}^{SF} \mathbf{y}[i, j] \cdot \mathbf{s}_1[j] + \sum_{j=1}^{SF} \mathbf{y}[i, j] \cdot \mathbf{x}_1[i-1, j]. \quad (22)$$

The only but quite important unknown is the adaptive orthogonal vector  $\mathbf{x}_1$ . Its derivation is introduced in [12], here only the results are presented

$$\mathbf{x}_1[i] = \mathbf{x}_1[i-1] - \mu \cdot Z[i] \cdot (\mathbf{y}[i] - Z_{MF}[i] \cdot \mathbf{s}_1). \quad (23)$$

The  $\mu$  value defines the algorithm step size. It can be set to  $\mu[i] = 1/i$ , then the algorithm converges to MMSE detector. In the case of multipath scenario, equation (23) changes to

$$\mathbf{x}_1[i+1] = (1 - \mu \cdot \nu_1) \cdot \mathbf{x}_1[i] - \mu \cdot Z[i] \times (\mathbf{y}[i] - Z_{MF}[i] \cdot \mathbf{s}_1) \quad (24)$$

where  $\nu_1$  is the Lagrangian multiplier chosen such that:

$$\sum_{j=1}^{SF} \mathbf{c}_1[j] \cdot \mathbf{c}_1[j] = \sum_{j=1}^{SF} \mathbf{x}_1[j] \cdot \mathbf{x}_1[j] + 1, \quad (25)$$

$$\sum_{j=1}^{SF} \mathbf{c}_1[j] \cdot \mathbf{s}_1[j] = 1. \quad (26)$$

### 4.2 Simulation Parameters

The program used for the simulation of the blind adaptive multiuser detection algorithm is the same as the one used for G-RAKE simulation, see subsection 2.3. All simulations were done with these parameters: spreading factor  $SF = 32$ , one realization with 2400 transmitted bits. Vector  $\mathbf{x}_1$  was the zero vector at the beginning of the simulation. After equation (28) was satisfied,  $\mathbf{x}_1$  was replaced by zero vector again. The Gram-Schmidt process was used (in each iteration) to ensure orthogonality condition between  $\mathbf{s}_1$  and  $\mathbf{x}_1$ . Step size  $\mu$  was set according to the stability condition, see [12]

$$\mu = \frac{1}{\sum_{k=1}^K A_k^2 + SF} \tag{27}$$

where  $K$  is the number of transmitting users in the system, and  $A_k$  is the received amplitude of user  $k$ .

$$\sum_{j=1}^{SF} \mathbf{x}_1[j] \cdot \mathbf{x}_1[j] \geq 5 \cdot \frac{K-1}{SF-(K-1)}. \tag{28}$$

All simulation results (figures) were approximated by polynomial functions.

## 5. Simulation Results

This section presents the results of the simulations performed. Some results have already been published in [13]. The aforementioned algorithms are compared with one another and also with the matched filter. BER (Bit Error Rate) was chosen as a parameter for the comparison of these algorithms.

### 5.1 G-RAKE Receiver

Fig. 5 shows a comparison of matched filter, RAKE receiver and G-RAKE receiver.

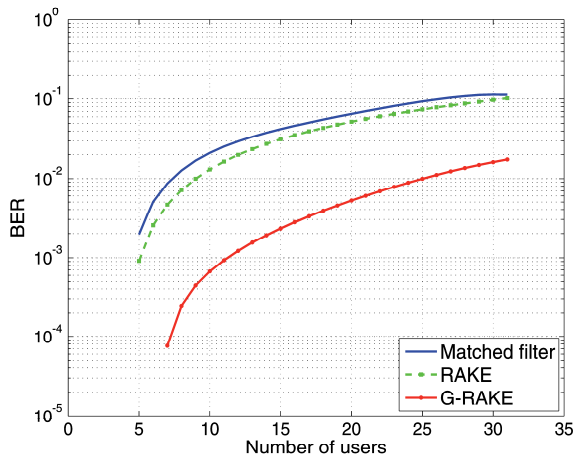


Fig. 5. Comparison of matched filter, RAKE and G-RAKE receiver.

A relationship between BER and the number of users in downlink is presented there. RAKE uses 3 fingers at 0, 1 and 2 chip period positions and its combining coefficients correspond with channel coefficients. The matched filter is placed at 0 chip period position. G-RAKE uses 4 fingers at -1, 0, 1 and 2 chip period positions and its combining coefficients are calculated by using (2). Fig. 5 shows that using a novel approach of computing the combining coefficients and only one extra finger at extra position, which does not match with any propagation path, enables increasing the system performance. By using G-RAKE instead of RAKE it is possible to decrease the BER or to increase the number of users in the system.

Fig. 6 shows a comparison of G-RAKE receiver performance for different numbers of fingers and for their different placements. G-RAKE *a* has 4 fingers at -1, 0, 1 and  $2 \cdot T_c$  (chip periods) positions. The other versions of G-RAKE are the same ones as G-RAKE *a* is, but they have some extra fingers. G-RAKE *b* has 1 extra finger at  $3 \cdot T_c$  position. G-RAKE *c* has 1 extra finger at  $-2 \cdot T_c$  position. G-RAKE *d* has 2 extra fingers at -2 and  $3 \cdot T_c$  positions. G-RAKE *e* has 2 extra fingers at -3 and  $-2 \cdot T_c$  positions.

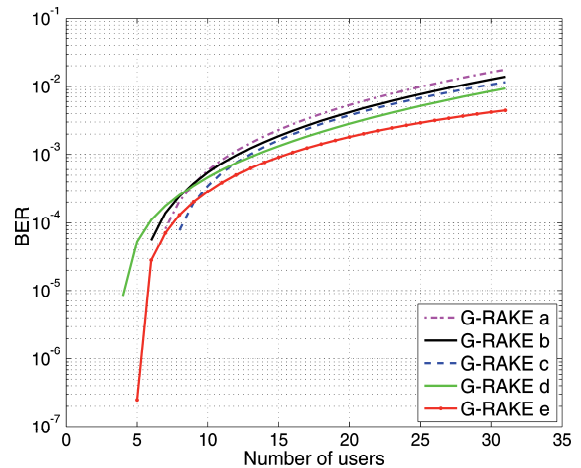


Fig. 6. Comparison of G-RAKE receiver performance for its different finger placements.

This simulation shows that increasing the number of fingers decreases BER. However, this need not be true in the case of good signal quality (low interference signal), where extra fingers may cause a slight decrease in performance. These extra fingers deal with signals that correspond to no multipath components and in the case of good signal quality they add noise. Fig. 6 also shows that a better performance can be achieved by using finger positions which were placed before channel delays.

Fig. 7 shows a comparison of G-RAKE receiver performance for different numbers of fingers and different numbers of channel paths. In this case, all paths were separated with one chip (delays were 0, 1, 2 and 3 chip periods) and their relative amplitudes were 0, -3, -8 and -12 dB. This simulation uses  $SF = 16$  and the constant

number of users = 15. The simulation shows that the maximum performance is achieved by using approximately twice as many fingers as channel paths, as given in [1]. Additional fingers do not increase the performance, or only very slightly, but they cause a sharp increase in computing power demands.

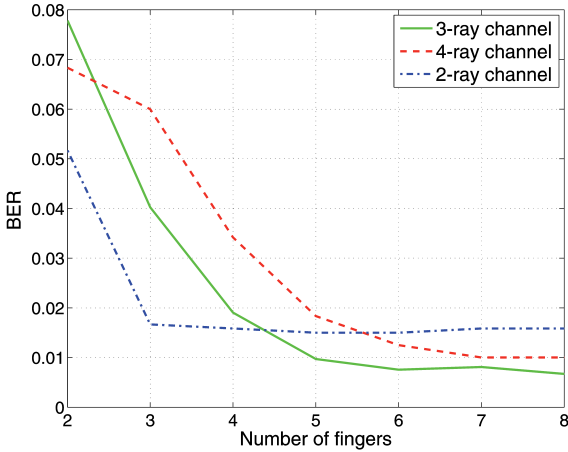


Fig. 7. Comparison of G-RAKE receiver performance for different multipath channels.

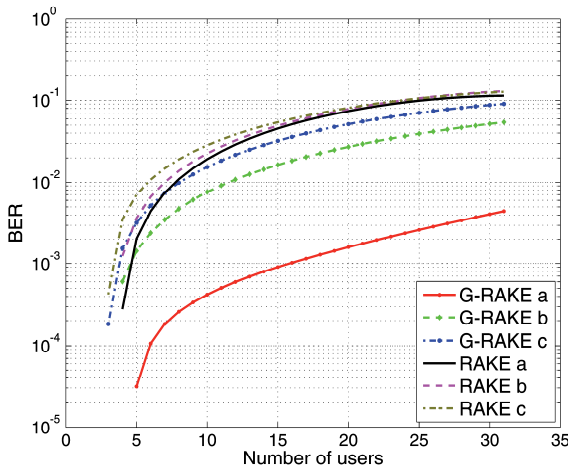


Fig. 8. RAKE and G-RAKE receiver performance for inexact channel estimates.

Fig. 8 shows a comparison between RAKE receiver and G-RAKE receiver for inexact channel estimates. In case *a* (RAKE *a* and G-RAKE *a*), the channel estimate is perfect. In case *b*, there is a 20% error of channel estimation (the values of relative amplitudes, which were used by the receiver, were decreased by 20%). And finally in case *c*, there is a 40% error of channel estimation. The simulation shows that G-RAKE is much more sensitive to inexact channel estimate than RAKE. It will be necessary to be careful of the channel estimate in order not to decrease the performance of the receiver.

### 5.2 Multiuser Detection

A comparison between matched filter and UMUD algorithm, see (14), is shown in Fig. 9. This simulation shows that it is possible to partially increase the system performance by using multiuser detection, even in the case when multipath scenario is not included in the system matrix.

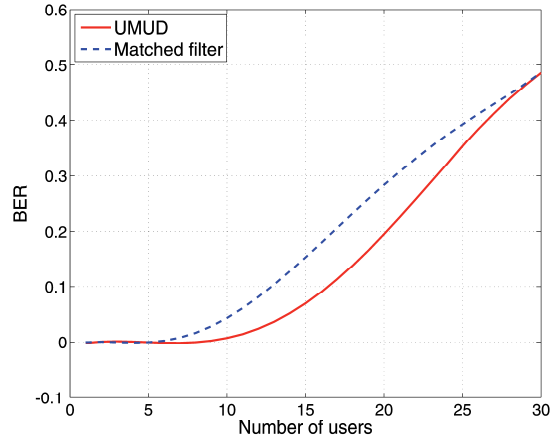


Fig. 9. Performance of UMUD algorithm.

A comparison between matched filter, UMUD algorithm, see (14), and UGMUD algorithm, see (18), is shown in Fig. 10. In this case, BER is a function of the number of neighboring cells; each cell contains two users. BER for all algorithms refers to the detection of both users in cell 1. Because the cell of interest contains a constant number of users (2 users), UMUD has only a slightly better performance than matched filter. If there were more users, its performance would be better. The UGMUD (its system matrix) involves also the detection of neighboring cells, so its performance is the best. This algorithm is quite complex and requires plenty of information about the system and its users, but it is able to significantly increase the system performance.

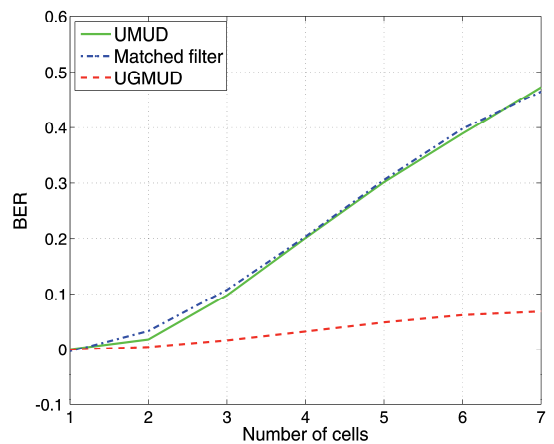


Fig. 10. Comparison of UMUD and UGMUD algorithms.

### 5.3 Blind Adaptive Multiuser Detection

A comparison between the conventional matched filter and the BMUD algorithm, see (22) and (24), is shown in Fig. 11. This figure shows the results for two types of the propagation channel. The first case (BMUD 1 and Matched filter 1) assumed an almost ideal channel. It had three paths. All paths were separated with one chip (delays were 0, 1 and 2 chip periods) and their relative amplitudes were 0, -40 and -43 dB. The second case (BMUD 2 and Matched filter 2) assumed the same channel which was introduced in subsection 2.3. The performance of BMUD is quite surprising. Its performance is worse than the performance of conventional matched filter in both cases. Note that the "Matched filter 1" curve is not visible in Fig. 11. This is because of the fact that BER of the matched filter is equal to zero in this case.

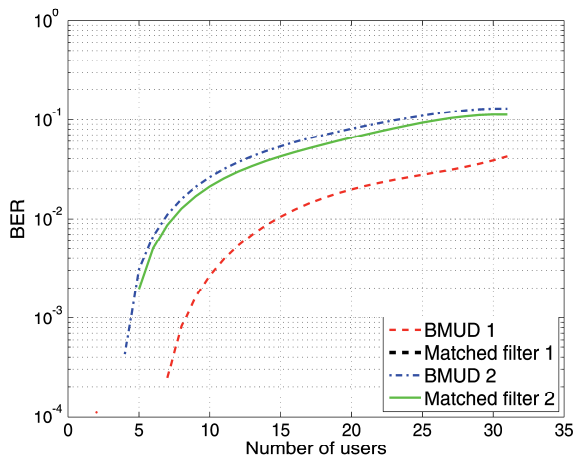


Fig. 11. Comparison of BMUD algorithm and matched filter for OVFS codes.

Fig. 12 shows a comparison between the conventional matched filter and the BMUD algorithm. Note the difference between Fig. 11 and Fig. 12 simulation parameters. The previous simulation, Fig. 11, uses orthogonal (OVFS) spreading codes (for channel coding). This simulation, Fig. 12, uses pseudorandom spreading codes. This figure shows the results for three types of the propagation channel. The first case (BMUD 1 and Matched filter 1) assumed an almost ideal channel. It is the same one as in the first case used for Fig. 11 (relative amplitudes were 0, -40 and -43 dB);  $\nu_1 = 0.01$ , see (24). The second case (BMUD 2 and Matched filter 2) assumed another type of multipath channel. It had three paths again. All paths were separated with one chip (delays were 0, 1 and 2 chip periods) and their relative amplitudes were 0, -9.1 and -11.4 dB;  $\nu_1 = 1.0$ . The third case (BMUD 3 and Matched filter 3) assumed the same channel which was introduced in subsection 2.3;  $\nu_1 = 10$ . Note that the "Matched filter 3" curve coincides with the "BMUD 3" curve and the "Matched filter 1" curve partially coincides with the "Matched filter 2" curve. Fig. 12 shows that the performance of BMUD is better than (or at least the same as) the performance of the

matched filter in all three cases. Fig. 12 also shows that the worse the channel is (the bigger relative amplitudes it has), the smaller the difference is between the matched filter and BMUD. Fig. 12 proves that BMUD is able to achieve a better performance than the conventional matched filter, but only for a special case of channel coding. It requires pseudorandom spreading codes. This feature makes it impossible to use this algorithm in modern systems, e.g. in UMTS.

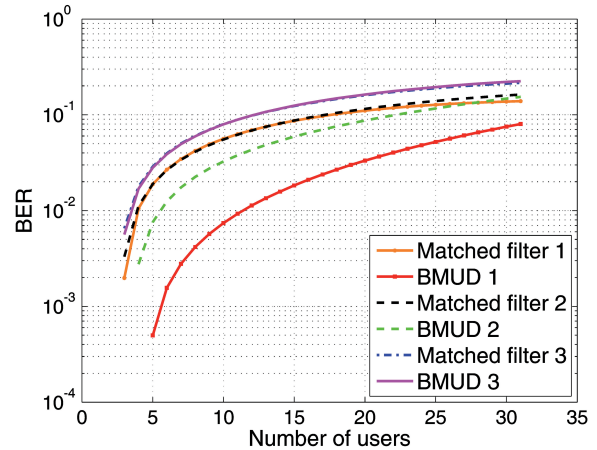


Fig. 12. Comparison of BMUD algorithm and matched filter for pseudorandom codes.

## 6. Conclusion

A brief description of the Generalized RAKE receiver, Uplink generalized multiuser detection, Blind adaptive multiuser detection and some simulation results were given in this contribution.

G-RAKE appears to be able to improve system capacity by using only a few additional fingers and a novel method of computing the combining coefficients. The maximum gain could be achieved by using twice as many fingers as channel paths. It should be noted that increasing the number of fingers means a bigger requirement for mobile station computing power. So the number of fingers will be a trade-off between the mobile station computing power and the required performance. G-RAKE is quite sensitive to inexact channel estimates, thus it will be necessary to be careful of this feature.

Uplink generalized multiuser detection appears to be able to improve the system capacity by providing joint detection of a great number of users in the system. The simulations introduced were partly simplified and thus the real properties and possible benefits of UGMUD should be verified by much more complex simulations or under real conditions.

Blind adaptive multiuser detection is able to give a better performance than the conventional matched filter, but only in the special case when pseudorandom spreading codes are used. Its performance is equal to the matched

filter performance or even worse when orthogonal spreading codes are used. This property makes it impossible to use this detector in systems like UMTS, for example.

Both above mentioned receivers (G-RAKE and UGMUD) appear to have potential benefits for CDMA systems, so their future research is recommended.

## Acknowledgements

This contribution has been supported by the research project of the GA CR (Czech Science Foundation) No. 102/07/1295 "Models of Mobile Networks and their Parts", by the research program No. MSM 0021630513 "Advanced Electronic Communication Systems and Technologies" (ELCOM), and by the project of the GA CR No. 102/08/H027 "Advanced Methods, Structures and Components of Electronic Wireless Communication".

## References

- [1] BOTTOMLEY, G., OTTOSSON, T., WANG, Y-P. A generalized RAKE receiver for interference suppression. *IEEE Journal on Selected Areas in Communications*, Aug. 2000, vol. 18, no. 8.
- [2] SUNDARARAJAN, J., MAHESHWARI, V., KOILPILLAI, R. Throughput enhancement in WCDMA using the generalized rake receiver. *IETE Journal of Research*, January 2005.
- [3] CAI, L., XU, Y., ZHANG, H., SONG, W. Performance of group ordered successive interference cancellation for multiuser detection in GSTBC SFH/MC DS-CDMA system. *Wireless Communications and Mobile Computing*, June 2006, vol. 6, pp. 475-482, DOI: 10.1002/wcm.290.
- [4] BENTRACIA, A., ZERGUINE, A., SHEIKH, A. Low-complexity linear group-SIC detectors. *Wireless Communications and Mobile Computing*, June 2007, vol. 7, pp. 595-604, DOI: 10.1002/wcm.374.
- [5] ZHENG, Z., YANG, Z., ZHU, Y., PAN, C. Channel estimation and interference suppression for uplink CDMA mobile communication systems. *Wireless Communications and Mobile Computing*, August 2004, vol. 4, pp. 483-489, DOI: 10.1002/wcm.191.
- [6] STAVROULAKIS, P. *Interference Analysis and Reduction*. Boston-London: Artech House, 2003. ISBN 1-580053-316-7.
- [7] The Generation Partnership Project Technical Specifications Group Radio Access Network Working Group 1. *BS Radio Transmission and Reception (FDD)*. TS 25.104 V5.3.0 (2002-06) [Online] Cited 2005-11-01. Document available at <http://www.3gpp.org/specs/specs.htm>.
- [8] JONES, A., WONG, S. Generalised multiuser detection in TD-CDMA. *IEEE Vehicular Technology Conference, VTC 2005 61st IEEE*, 2005, vol. 3. ISSN 1550-2252.
- [9] MAO, Z., BHARGAVA, V. Fast converging adaptive MMSE multiuser detector for DS-CDMA system. *Wireless Personal Communications*, January 2005, vol. 32, no. 2. ISSN 0929-6212.
- [10] SAAIFAN, K., HASSAINI, E. Diversity reception of an asynchronous blind adaptive multiuser detector through correlated Nakagami fading channel. *Wireless Personal Communications*, March 2007, vol. 40, no. 4. ISSN 0929-6212.
- [11] HMIDAT, A., SHARIF, B., WOO, W., HASSAN, M. Fuzzy-based multiuser detector for impulsive CDMA channel. *European Transactions on Telecommunications*, November 2007, vol. 18, pp. 769-776, DOI: 10.1002/ett.1244.
- [12] HONIG, M., MADHOW, U., VERDU, S. Blind adaptive multiuser detection. *IEEE Transactions on Information Theory*, July 1995, vol. 41, no. 4.
- [13] KEJÍK, P., HANUS S. Interference cancellation in 3G systems. In *Proceedings of the Sixteenth International Electrotechnical and Computer Science Conference ERK 2007* (ISSN 1581-4572). Portoroz (Slovenia): Slovenia Section IEEE, Ljubljana University, 2007, p. 257-260.

## About Authors ...

**Petr KEJÍK** received the BSc degree in 2005 and the MSc degree in 2007 from Brno University of Technology, Department of Radio Electronics, Brno, Czech Republic. In 2007, he started studies towards a PhD degree at the same university. His research interests include capacity and access optimization in CDMA systems.

**Stanislav HANUS** was born in Brno, Czech Republic, in 1950. He received the MSc and PhD degrees from Brno University of Technology. He is Professor at the Department of Radio Electronics, Faculty of Electrical Engineering and Communication in Brno. His research is concentrated on Mobile Communications and Television Technology.